Journal of
Plankton Research

plankt.oxfordjournals.org

J. Plankton Res. (2014) 36(6): 1423–1433. First published online August 11, 2014 doi:10.1093/plankt/fbu069

Evaluation of the utility of xanthophyll cycle pigment dynamics for assessing upper ocean mixing processes at Station ALOHA

ROBERT R. BIDIGARE[1,2]*, FENINA R. BUTTLER[1], STEPHANIE J. CHRISTENSEN[1], BENEDETTO BARONE[2], DAVID M. KARL[2] AND SAMUEL T. WILSON[2]

[1]HAWAII INSTITUTE OF MARINE BIOLOGY, UNIVERSITY OF HAWAII, PO BOX 1346, KANEOHE, HI 96744, USA AND [2]DANIEL K. INOUYE CENTER FOR MICROBIAL OCEANOGRAPHY: RESEARCH AND EDUCATION, UNIVERSITY OF HAWAII, 1950 EAST-WEST ROAD, HONOLULU, HI 96822, USA

*CORRESPONDING AUTHOR: bidigare@hawaii.edu

Received April 17, 2014; accepted July 7, 2014

Corresponding editor: Zoe Finkel

We had the opportunity to evaluate the utility of the chromophyte xanthophyll cycle pigments (XCP), diadinoxanthin (DDX) and diatoxanthin (DTX), for assessing upper ocean mixing processes at Station ALOHA (22.75°N, 158°W) during August–September 2012. De-epoxidation state (DES, [DTX]/[DDX + DTX]) kinetic rate experiments were performed that quantified the conversion of DDX to DTX in the light. DES values ranged from 0.13 to 0.51 (weight: weight), and yielded a first-order rate constant of 0.16 ± 0.02 min^{-1}. In addition, a time-series of chromophyte pigments was collected from the sea-surface in order to quantify the time-dependent rate of change in the ratio of XCP to chlorophyll *a* (XCP/CHLA). *In situ* XCP/CHLA values were measured by rapid collection of cells in the mixed layer using a diaphragm pumping system and the xanthophyll cycle activity inhibitor dithiothreitol. Turbulent transfer velocity (TTV) was estimated as the quotient of the XCP/CHLA photoadaptation rate and the XCP/CHLA gradient in the mixed layer. TTVs ranged from 0.3 to 0.5 cm s^{-1}, and agreed to within a factor of ~2 of the Lagrangian float-derived estimate of vertical mixing at a comparable friction velocity. Coincident measurements of dissolved gases suggest that XCP dynamics may be useful for the interpretation of trace gases species distributions, such as hydrogen and carbon monoxide, in the upper ocean.

KEYWORDS: upper ocean mixing; xanthophyll cycle; station aloha; diadinoxanthin; diatoxanthin; hoe-dylan

available online at www.plankt.oxfordjournals.org

INTRODUCTION

Turbulent mixing in the upper ocean is driven by a variety of air–sea interactions including, but not limited to, Ekman transport, evaporative and nighttime cooling that creates vertical convection, wind-driven currents that produce friction velocities, wave–current interactions that generate Langmuir circulation cells and wave breaking that produces bubbles and turbulence. Upper ocean mixing processes are important because they provide a link between the atmosphere and the deep ocean, and are responsible for the air–sea exchange of freshwater, heat, momentum and gases. The measurement and modeling of boundary layer turbulence in the ocean is challenging because it varies by several orders of magnitude. Consequently, a wide variety of approaches have been used to study upper ocean turbulence including acoustic drifters, thermistor strings, free fall airfoil probes, Doppler profilers, Lagrangian drifters and large-eddy simulations (Gargett, 1997).

Turbulent mixing also influences predator–prey interactions and particle aggregation, and controls the availability of new nutrients and photosynthetically active radiation (PAR, 400–700 nm) in the euphotic zone (Gargett, 1997). Consequently, turbulence has a profound effect on phytoplankton distributions, abundances, rates of carbon fixation and photoadaptation state. This subject matter resulted in the publication of a number of seminal papers in the 1980s (Cullen and Lewis, 1988; Denman and Gargett, 1983; Lewis *et al.*, 1984) and continues to be an active area of research as evidenced by recent publications and ongoing research efforts. In particular, knowledge of photoadaptation rate kinetics and *in situ* measurements of photoadaptation state have been used to estimate (or constrain) rates of vertical mixing in the upper ocean (Brunet *et al.*, 2003, 2008; Dusenberry, 1995; Dusenberry *et al.*, 1999; Griffith *et al.*, 2010).

Phytoplankton utilize a wide variety of mechanisms for adapting to the variable light field experienced in the upper ocean. The timescales for the pigment-based adaptations range from seconds–minutes in the case of xanthophyll cycling (XC), minutes–hours for the synthesis of photoprotective carotenoids and hours–days for the synthesis of light harvesting pigments (Ferris and Christian, 1991). For certain chromophytic microalgae (diatoms, xanthophytes, raphidophytes, euglenophytes, pelagophytes, prymnesiophytes and dinoflagellates; Brunet *et al.*, 2011), the XC involves the reversible interconversion of diadinoxanthin (DDX) and diatoxanthin (DTX). The de-epoxidation reaction (DDX→DTX) follows first-order kinetics and can be modeled using the following equation (Griffith *et al.*, 2010):

$$-kt = \ln[(\mathrm{DES_t} - \mathrm{DES_\infty})/(\mathrm{DES_o} - \mathrm{DES_\infty})] \quad (1)$$

where DES is the de-epoxidation state and defined as [DTX]/[DTX + DDX] (dimensionless), k is the first-order rate constant (min^{-1}), $\mathrm{DES_o}$ is the initial dark-adapted DES value, DES_t is the DES value at time t (min) and $\mathrm{DES_\infty}$ is the DES value when pigment changes follow zero-order kinetics (i.e. the light-adapted DES value). Laboratory-based experiments performed with diatom cultures yield rate constants ranging from 0.1 to 0.3 min^{-1} DDX → DTX (Kashino and Kudoh, 2003; Lohr and Wilhelm, 1999; Olaizola and Yamamoto, 1994). In contrast, the epoxidation reaction (DTX→DDX) is considerably slower with rate constants ranging from 0.01 to 0.06 min^{-1} (Kashino and Kudoh, 2003; Lohr and Wilhelm, 1999). XC activity is an important mechanism responsible for non-photochemical quenching (NPQ) and is correlated with decreases in the efficiency of maximum quantum yield for photosystem II activity (i.e. $\mathrm{F_v/F_m}$) as measured by active fluorescence (Brunet and Lavaud, 2010).

Based on a combined approach involving metabolite analysis identification of gene function with the model diatom *Phaeodactylum tricornutum*, Dambek *et al.* (Dambek *et al.*, 2012) determined that DDX and fucoxanthin are synthesized from β,β-carotene via the following pathway:

$$\begin{aligned}\beta,\beta-\text{carotene} &\rightarrow \text{Zeaxanthin} \rightarrow \text{Antheraxanthin}\\ &\rightarrow \text{Violaxanthin}\\ &\rightarrow \text{Neoxanthin}\begin{cases}\nearrow \text{Diadinoxanthin}\\ \searrow \text{Fucoxanthin}\end{cases}\end{aligned}$$

Lepetit *et al.* (Lepetit *et al.*, 2010) determined that the marine diatom, *Cyclotella meneghiniana*, has three different DDX+DTX pools that are associated with: (i) the peripheral fucoxanthin chlorophyll protein (FCP) complexes, (ii) the FCP complexes bound to photosystem I (PSI), and (iii) a monogalactosyldiacyl–glycerol (MGDG) lipid shield surrounding the peripheral FCP complexes. The first two pools are relatively small and do not vary under changing light conditions. Lepetit *et al.* (Lepetit *et al.*, 2010) suggest that the peripheral FCP XC pool is involved in NPQ, and the PSI XC pool is involved in light harvesting and the detoxification of triplet chlorophyll (^{3}Chl) and singlet oxygen ($^1\mathrm{O_2}$). The third pool accounts for the majority of DDX + DTX and increases under high light. Lepetit *et al.* (Lepetit *et al.*, 2010) hypothesize that DTX in the lipid-dissolved XC pool functions as an antioxidant by scavenging $^1\mathrm{O_2}$ and peroxylipids. Measurements of xanthophyll cycle pigments (XCP) have been used in field studies for assessing phytoplankton light histories (Bidigare *et al.*, 1987; Claustre *et al.*, 1994; Olaizola *et al.*, 1992) and photoadaptation strategies (Brunet *et al.*, 2008; Kashino *et al.*, 2002),

water column stability (Moline, 1998), mixing rates in the upper ocean (Brunet *et al.*, 2003, 2008; Griffith *et al.*, 2010; Welschmeyer and Hoepffner, 1986) and the depth of origin of sinking particulate organic matter (Scharek *et al.*, 1999).

During May–October of 2012, the Center for Microbial Oceanography: Research and Education (C-MORE, University of Hawaii) conducted a "continuous" long-term field experiment (HOE-DYLAN: Hawaii Ocean Experiment—Dynamics of Light and Nutrients) at Station ALOHA to observe and interpret temporal variability in microbial processes, and the consequences for ecological dynamics and biogeochemical cycling. Special focus was given to time-space coupling because proper scale sampling of the marine environment is an imperative, but generally neglected aspect of marine microbiology. We had the opportunity to investigate time- and depth-dependent changes in phytoplankton pigments during 22 August–11 September 2012 (Cruise ID: KM1219). The primary objective of our research component was to evaluate the utility of XCP dynamics as a chemical tracer of vertical mixing processes.

METHOD

Laboratory investigation of dithiothreitol inhibition

Since the interconversion of XCP occurs on timescales of seconds–minutes, previous studies have employed the use of the XC activity inhibitor, dithiothreitol, in order to obtain reliable first-order rate constants (Kashino and Kudoh, 2003; Lavaud *et al.*, 2002; Olaizola and Yamamoto, 1994). Prior to the field studies, a laboratory experiment was performed to determine the concentration of dithiothreitol (DTT) required for the inhibition of XC activity. A unialgal culture of *Pelagomonas* sp., isolated from Station ALOHA by Yoshimi Rii (University of Hawaii), was used in the DTT exposure experiment. The culture was dark-adapted overnight at room temperature. The following morning, 25 mL culture aliquots were dispensed into 75-cm^2 cell culture flasks under dim red lighting. One flask ("dark control") was immediately filtered onto a 25 mm diameter Whatman GF/F filter (nominal porosity of 0.7 μm) under dim light and frozen at −20°C. DL-Dithiothreitol was obtained from Sigma-Aldrich and used to prepare a 50 mM stock solution. With the exception of one of the remaining samples ("light control"), DTT was added to the individual flasks under dim red lighting; the final concentrations ranged from 50 to 495 μM DTT. The samples were allowed to sit in the dark for 30 min. The flasks were then exposed to an irradiance of 300 μmol quanta m^{-2} s^{-1} (400–700 nm) for 30 min at 25°C in a Percival model E22L incubator. The samples were immediately filtered onto 25 mm diameter Whatman GF/F filters under dim light and frozen at −20°C. Samples were extracted overnight and analyzed the following day by the high-performance liquid chromatography (HPLC) using the procedure described below.

Study site and hydrography

Field studies were conducted aboard the R/V *Kīlo Moana* at Station ALOHA (22.75°N, 158°W) during KM1219 (22 August–11 September 2012). Conductivity–temperature–depth (pressure) measurements were performed with a Sea-Bird SBE 911plus CTD system attached to a rosette of 24 × 12-L polyvinyl chloride sample bottles. The conductivity sensor was calibrated using discrete sample salinity measurements as described by Bingham and Lukas (Bingham and Lukas, 1996). Mixed layer depths (m) were defined using a density offset of 0.03 kg m^{-3} from a depth of 10 m (de Boyer Montégut *et al.*, 2004). Vertical profiles of downwelling PAR irradiance were obtained every day using a Free-Falling Optical Profiler (Satlantic). A deck sensor by the same manufacturer was mounted on the upper deck of the ship and measured downwelling PAR at the sea surface while the vertical profiles were recorded. Both these measurements were used to compute the percent level of PAR with respect to the value at the sea surface on 1 m depth bins in the water column.

Meteorological data were obtained from the Woods Hole Oceanographic Institution—Hawaii Ocean Time-series Site (WHOTS, http://www.soest.hawaii.edu/whots/) mooring located near Station ALOHA (22.77°N, 157.90°W). The mooring has been in place for 1-year periods since 2004. Data for this study were acquired during the WHOTS-9 deployment (14 June 2012–14 July 2013). The WHOTS surface buoy is equipped with meteorological instrumentation that measured air and sea-surface temperatures, relative humidity, barometric pressure, wind speed and direction, incoming shortwave and long-wave radiation, and precipitation. Wind speed (m s^{-1}) data were measured at a height of 3.3 m during 1100–1500 HST, and were used to calculate values at 15 m (U_{15}, m s^{-1}) and corresponding friction velocities (u_*, m s^{-1}) as described in D'Asaro (D'Asaro, 2001).

Field studies of XCP kinetics

DES kinetic rate parameter experiments were performed on 24 and 30 August (KM1219). Sea-surface water samples were collected with an 8-L plastic bucket at ~1000 HST (PAR = 1280–1300 μmol quanta s^{-1}

m^{-2}) and transferred to a 20-L clear, UV-opaque, polycarbonate carboy. The carboy was wrapped in a black plastic bag and placed into a Rubbermaid Action Packer storage container. A Biospherical Instruments model QSL-2100 radiometer was used to measure the PAR irradiance inside of the dark incubator and yielded a value of 0 μmol quanta m^{-2} s^{-1}. After a dark adaption period of 60 min in the shade, the carboy was placed in direct sunlight and samples were collected at 0, 1, 2, 3, 4, 5, 10, 15, 30 and 45 min ($n = 10$ samples). Single 2.16-L samples were directly dispensed into opaque sample bottles containing DTT to rapidly inhibit XC activity. Samples were filtered onto 25 mm diameter Whatman GF/F filters, flash-frozen in liquid nitrogen and then stored in the −80°C shipboard freezer. Samples were transported to the University of Hawaii on dry ice, and stored at −80°C prior to analysis using the HPLC method described below. The results of these experiments were combined and modeled using Eq. (1). Linear regression analysis and the standard error of the resulting slope were obtained using Minitab 13 statistical software.

Phytoplankton pigment time-series measurements

A time-series of phytoplankton chlorophyll and carotenoid pigments was collected from the surface waters (5 m) of Station ALOHA during 23 August to 7 September. Seawater was collected at 1200 or 1600 HST using the CTD-rosette system described above. Single 2.16-L samples were filtered onto 25 mm diameter Whatman GF/F filters, flash-frozen in liquid nitrogen and then stored in the −80°C shipboard freezer. Samples were transported to the University of Hawaii on dry ice, and stored at −80°C prior to analysis using the HPLC method described below.

A second time-series of phytoplankton pigments was collected from the surface waters of Station ALOHA during 5 and 6 September. Hourly bucket samples were collected during daylight hours (dawn to dusk). Sea-surface irradiance was continuously measured during the cruise using a Biospherical Instruments model QSR-2200 PAR sensor mounted on the mast of the R/V *Kilo Moana*. Bucket samples were transferred into 2-L opaque sample bottles containing DTT to rapidly inhibit XC activity. Replicate samples were collected on 6 September under low-light (0646 HST, PAR = 400 μmol quanta s^{-1} m^{-2}, $n = 4$) and high-light (1415 HST, PAR = 700 μmol quanta s^{-1} m^{-2}, $n = 4$) conditions to assess the variability associated with the HPLC pigment determinations. Single 2.16-L samples were filtered onto 25 mm diameter Whatman GF/F filters, flash-frozen in liquid nitrogen and then stored in the −80°C shipboard freezer. Samples were transported to the University of Hawaii on dry ice, and stored at −80°C prior to analysis using the HPLC method described below.

Chromophyte pigment vertical profile measurements

Samples for determining vertical profiles of phytoplankton pigments during KM1219 were collected with a Wilden diaphragm pumping system equipped with ~75 m of Teflon® tubing that was labeled in 5 m increments. The pumping system was deployed during 1400–1500 HST and 10 samples were collected at 5 m intervals in the upper 50 m. The calculated residence time of seawater in the tubing was 1.2 min. After flushing the tubing for 3 min, samples were directly dispensed into 2-L opaque sample bottles containing DTT to rapidly inhibit XC activity. Single 2.16-L samples were filtered onto 25 mm diameter Whatman GF/F filters, flash-frozen in liquid nitrogen and then stored in the −80°C shipboard freezer. Samples were transported to the University of Hawaii on dry ice, and stored at −80°C prior to analysis using the HPLC method described below. Average downwelling PAR at the sea-surface was measured every 10 min during the diaphragm-pump vertical casts using a LI-COR model LI-192 cosine collector mounted on the top deck of the R/V *Kilo Moana*. Mixed layer depth (m) was estimated as the mean of the values determined before (1200 CTD cast) and after (1600 CTD cast) a given vertical profiles.

Phytoplankton pigment measurements

Chlorophyll and carotenoid pigments were analyzed at the University of Hawaii using the HPLC method described by Bidigare *et al.* (Bidigare *et al.*, 2005). Pigment samples were extracted at 4°C in the dark for 24 h in 3 mL of 100% HPLC grade acetone (Fisher Scientific) plus an internal standard (50 μL canthaxanthin). After extraction, samples were centrifuged (5 min at 1500 × *g*) to sediment filter and cellular debris. Samples of a mixture of 0.3 mL HPLC grade water (Fisher Scientific) plus 1.0 mL extract were injected onto a Varian 9012 HPLC system equipped with a Varian 9300 autosampler, a Timberline column heater (26°C) and Spherisorb 5 μm ODS2 analytical (4.6 × 250 mm) column and corresponding guard cartridge. Pigments were detected with a ThermoSeparation UV2000 detector (λ = 436 nm and 450 nm). A ternary solvent system was employed for HPLC pigment analysis: eluent A (MeOH:0.5 M ammonium acetate, 80:20), eluent B (acetonitrile:water, 87.5:12.5) and eluent C (ethyl acetate). The linear

gradient used for pigment separation is a modified version of that originally described by Wright *et al.* (Wright *et al.*, 1991): $t = 0$ min (90% A, 10% B), $t = 1$ min (100% B), $t = 11$ min (78% B, 22% C), $t = 27.5$ min (10% B, 90% C) and $t = 29$ min (100% B). Eluents A and B contain 0.01% of 2,6-di-tert-butyl-p-cresol (Sigma-Aldrich) to prevent the conversion of chlorophyll *a* into chlorophyll *a* allomers. HPLC grade solvents (Fisher Scientific) were used to prepare eluents A, B and C. The eluent flow rate was held constant at 1 mL min^{-1}. Pigment peaks were identified by comparing their retention times with those of pigment standards provided by DHI Lab Products (Hørsholm, Denmark; http://c14.dhigroup.com/ProductDescriptions/PhytoplanktonPigmentStandards.aspx) and extracts prepared from phytoplankton reference cultures. Pigment concentrations were calculated using internal and external standards, and expressed as concentrations (ng pigment per L of filtered seawater) or pigment ratios (weight:weight).

Trace gas measurements

To assess the applicability of upper-ocean mixing estimates, vertical profiles of two dissolved gases; hydrogen (H_2) and carbon monoxide (CO) were conducted at 10 m intervals within the upper 80 m of the water column. The sampling procedures and analytical methods were identical to those previously described at Station ALOHA (Blomquist *et al.*, 2012; Wilson *et al.*, 2013). Seawater samples were collected using a rosette of 12-L polyvinyl chloride sample bottles and transferred to acid-washed, combusted, glass stoppered 300 mL Wheaton bottles. Dissolved H_2 and CO concentrations were determined onboard immediately using headspace equilibration and all samples were analyzed within 1.5 h of collection. The headspace equilibration was conducted using a 50 mL gas-tight, glass syringe (Perfektum) which was contained within a custom-built syringe actuator to ensure accurate and reproducible volumes were used for each sample analysis. The equilibrated headspace was injected into the inlet of the reduced gas analyzer (Peak Laboratories; Mountain View, CA) as previously described (Xie *et al.*, 2002). H_2 and CO were chromatographically separated from other gases using a dual column system (packed Unibeads 1S 60/80 mesh, 3.2 mm diameter and 42 cm length and Molecular Sieve 13X, 60/80 mesh, 3.2 mm diameter and 206 cm length) maintained at 104°C. The sample gas stream subsequently passed through a heated mercuric oxide bed (250°C) to produce mercury vapor which was quantified using an UV absorption photometer located immediately downstream from the reaction site. The retention time for H_2 and CO with a carrier gas flow rate of 20 mL min^{-1} was 45 and 112 s, respectively. The system was calibrated using serial dilutions of a 1 ppmv ± 1% H_2 gas standard and a 5 ppmv ± 1% CO gas standard (Scott Marrin).

RESULTS AND DISCUSSION

Inhibition of XC activity by DTT

The results of the *Pelagomonas* sp. XC activity experiment are shown in Fig. 1. The dark- and light-control flasks yielded DES values of 0.03 and 0.33, respectively. DES values decreased monotonically at inhibitor concentrations ranging from 50 to 200 μM DTT, and remained low and constant at higher DTT concentrations. These findings are similar to those of Lavaud *et al.* (Lavaud *et al.*, 2002) and Kashino and Kudoh (Kashino and Kudoh, 2003) who reported that XC activities were completely inhibited at inhibitor concentrations of ≥200 μM DTT. Based on these results, we used a final DTT concentration of 300 μM to ensure a complete inhibition of XC activity in the seawater samples collected during KM1219.

XCP kinetics

The results of the DES kinetic rate parameter experiments are shown in Fig. 2a. DES values ranged from 0.13 to 0.51 during these experiments. DES_o and DES_∞ values of 0.00 and 0.59, respectively, were obtained from the chromophyte pigment time-series described below. These results were modeled using first-order kinetics (Griffith *et al.*, 2010) and yielded a rate constant of 0.16 ± 0.02 min^{-1} (Fig. 2b). This value falls within the range of those determined in laboratory experiments performed with diatoms (0.09–0.28 min^{-1}, Table I).

Phytoplankton pigment time-series

A time-series of phytoplankton pigment concentrations measured at a depth of 5 m during 23 August–7 September 2012 is shown in Fig. 3. While time-dependent changes

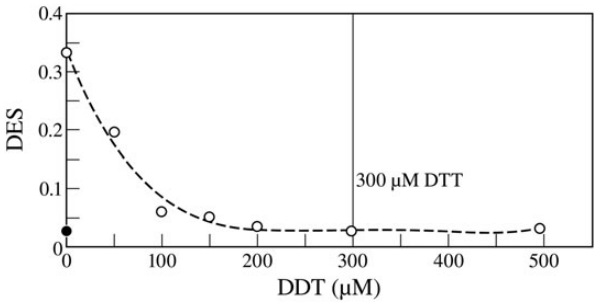

Fig. 1. Inhibition of XC activity in *Pelagomonas* sp. by dithiothreitol (filled circle = dark control flask and open circle = light-exposed flasks).

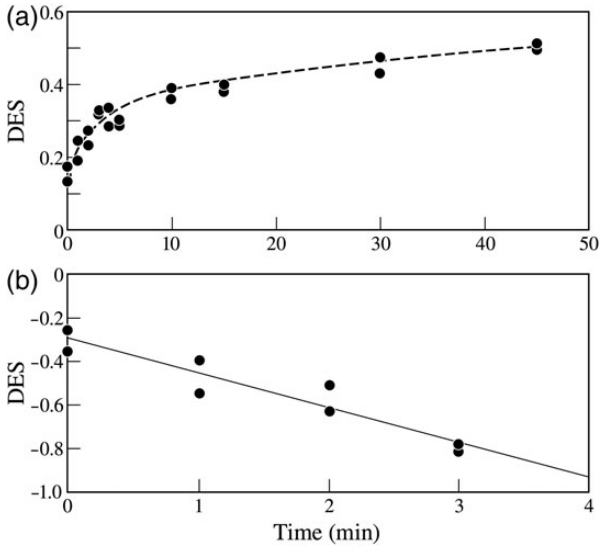

Fig. 2. De-epoxidation state (DES) kinetic experiments performed with natural chromophyte populations sampled from surface waters during KM1219: (**a**) DES vs. time and (**b**) LN DES ratio vs. time.

Table I: Comparison of rate constants (k_1) for the conversion of DDX to DTX by diatoms and mixed populations of chromophyte microalgae

k_1 (min^{-1})	Sample ID	Reference
0.16 ± 0.02	Chromophytes	This study
0.09–0.13	*P. tricornutum*	Olaizola and Yamamoto (1994)
0.10–0.20	*C. gracilis*	Kashino and Kudoh (2003)
0.25–0.28	*P. tricornutum*	Lohr and Wilhelm (1999)

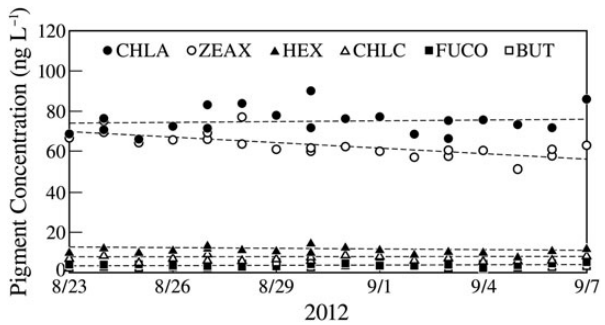

Fig. 3. Phytoplankton pigment time-series measured at a depth of 5 m during KM1219 (see text for details).

in CHLA, chlorophyll *c* (CHLC), fucoxanthin (FUCO, diatom biomarker), 19′-butanoyloxyfucoxanthin (BUT, pelagophyte biomarker) and 19′-hexanoyloxyfucoxanthin (HEX, prymnesiophyte biomarker) concentrations were not significant ($P > 0.100$), Zeaxanthin (ZEAX, cyanobacteria biomarker) concentrations decreased significantly during the course of cruise KM1219 ($P < 0.001$). The decrease in the latter was associated with a decline in the abundance of *Prochlorococcus* spp. as measured by flow cytometry (data not shown). These findings suggest that the chromophytic microalgae populations remained relatively constant during KM1219.

At Station ALOHA, the dominant chromophytic microalgae that possess a DDX-DTX xanthophyll cycle include the diatoms, pelagophytes and prymnesiophytes (Andersen *et al.*, 1996). The sum of the photosynthetic carotenoids (PSC), FUCO, BUT and HEX is used as a biomarker for chromophytic microalgae, and XCP is defined as the sum of DDX and DTX. In order to adjust for temporal changes in phytoplankton pigment biomass during KM1219, PSC and XCP concentrations are normalized to chlorophyll *a* (CHLA). The respective uncertainties of the HPLC-determined PSC, XCP, PSC/CHLA and XCP/CHLA values are ±5.7, ±6.1, ±5.6 and ±6.0%, and used to construct the error bars in Fig. 3.

XCP concentrations increased during 0700 to 1000, remained constant during 1000 to 1500 and decreased during 1500 to 1900 (Fig. 4a). Concentrations of PSC remained relatively constant during the daylight hours. XCP/CHLA values increased from 0700 to 1100 HST, remained constant during 1100 to 1500 HST and decreased from 1500 to 1900 HST (Fig. 4b). It is interesting to note that XCP/CHLA values were similar on 5 and 6 September despite the ∼two-fold difference in PAR. The maximum XCP/CHLA values (0.180–0.182) were measured during 1200–1400 HST, and the minimum XCP/CHLA values (0.075–0.084) were measured during 0700–0800 HST. These latter values are in good agreement with nighttime observations (5 m, 2000 HST) during June–September at Station ALOHA during 1989–2011 (0.079 ± 0.004, http://hahana.soest.hawaii.edu/hot/hot-dogs/). PSC/CHLA values remained relatively constant during the daylight hours.

Rates of photoadaptation (ΔXCP/CHLA per unit time = dP/dt) were estimated via linear regression analysis of the data in Fig. 4b. The slopes of these data averaged $6.7 \pm 0.5 \times 10^{-6}$ s^{-1} (Fig. 5) for XCP/CHLA increases and decreases on 5 and 6 September. It should be noted that these photoadaptation rates may be slightly underestimated (morning samples) or overestimated (afternoon samples) since the surface bucket samples were already subjected to natural mixed layer mixing. Despite this uncertainty, the rates reported here are in very good agreement with those determined during the light shift experiments performed by Harris *et al.* (Harris *et al.*, 2009) with *Emiliania huxleyi* (dP/dt = $5.6 \pm 1.4 \times 10^{-6}$ s^{-1}; see their Fig. 3c).

Chromophyte pigment vertical profiles

Five vertical profiles were conducted using the diaphragm pump during 26 August–1 September, and surface PAR

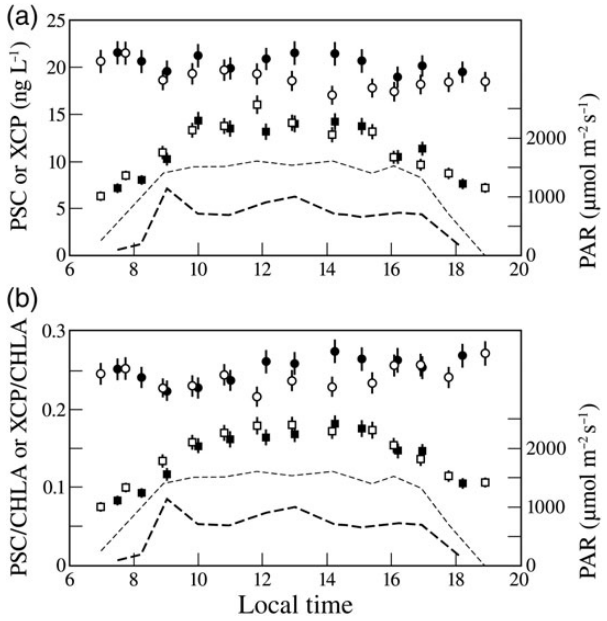

Fig. 4. Chromophyte pigment time-series measured during KM1219: (**a**) photosynthetic carotenoid concentrations (PSC, open circle: 5 September and filled circle: 6 September) and xanthophyll cycle pigment concentrations (XCP, open square: 5 September and filled square: 6 September) and (**b**) chlorophyll *a*-normalized photosynthetic carotenoid concentrations (PSC/CHLA, open circle: 5 September and filled circle: 6 September) and chlorophyll *a*-normalized xanthophyll cycle pigment concentrations (XCP/CHLA, open square: 5 September and filled square: 6 September). Note that the irradiance on 5 September (dotted line) was approximately two-fold higher than that measured on 6 September (dashed line).

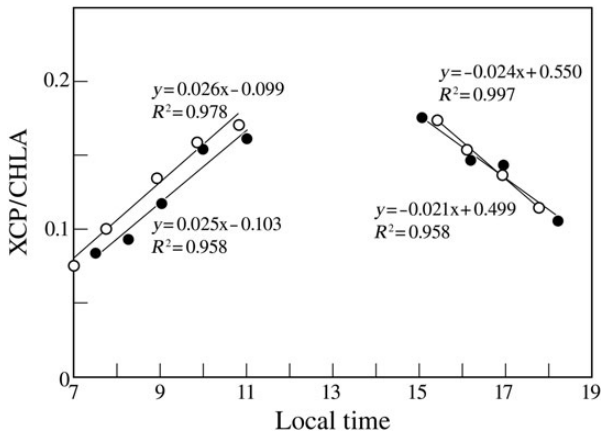

Fig. 5. Rates of photoadaptation measured on 5 September (open circle) and 6 September (filled circle) during KM1219.

averaged 1383 ± 140 μmol quanta m^{-2} s^{-1} (± 10%) during these casts (Table II). Mixed layer depths and wind speeds (U_{15}) ranged from 18 to 45 m and 7.4 to 9.1 m s^{-1}, respectively. Vertical profiles XCP/CHLA are presented in Fig. 6. Values are expressed as a function of normalized

Table II: Surface irradiance fluxes (μmol quanta m^{-2} s^{-2}), mixed layer depths (MLD), wind speeds (U_{15}), friction velocities (u_*), turbulent transport velocities (TTV) and mixing timescales (T) for the XCP pump casts performed during KM1219

Date	PAR	MLD (m)	U_{15} (m s^{-1})	u_* (m s^{-1})	TTV (cm s^{-1})	T (h)
26 August	1522	18	7.5	0.0089	0.00	∞
28 August	1177	29	7.7	0.0091	0.37	2.2
29 August	1314	45	9.0	0.0107	0.29	4.3
31 August	1418	40	8.9	0.0106	0.52	2.2
1 September	1484	27	8.0	0.0095	0.48	1.6

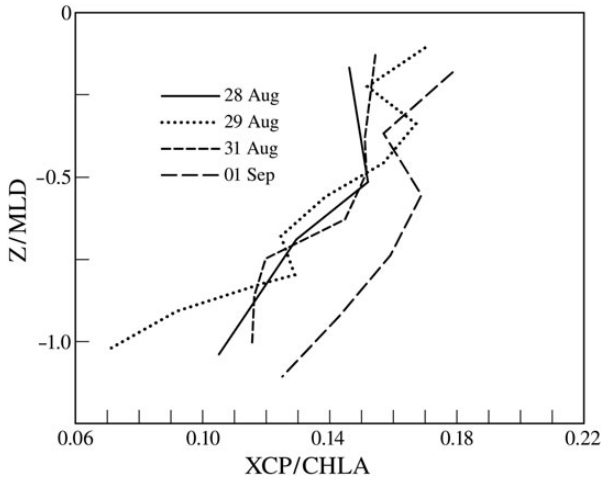

Fig. 6. Pump profiles of normalized XCP-to-CHLA ratios (Z/MLD = sample depth (m)/mixed layer depth (m), dimensionless) measured during KM1219.

mixed layer depth (i.e. z/MLD, dimensionless in order to facilitate the comparison of data collected on different days). The observed vertical distributions of XCP/CHLA shown are dependent upon both photoadaptation and mixing processes (Cullen and Lewis, 1988; Lewis *et al.*, 1984), and the water motions responsible for XCP dynamics are collectively referred to as a turbulent transfer velocity (TTV).

Estimation of turbulent transfer velocities

A summary of the wind-forcing and mixing parameters used to estimate turbulent transfer velocities during KM1219 are presented in Table III. TTV (dz/dt, cm s^{-1}) was estimated as the quotient of the XCP/CHLA photoadaptation rate (6.7×10^{-6} s^{-1}) and the XCP/CHLA gradient in the mixed layer (cf. Fig. 6):

$$\mathrm{TTV} = (dP/dt)(dP/dz)^{-1} \qquad (2)$$

Table III: Summary of the wind-forcing and mixing parameters used in the analysis of KM1219 data

Parameter	Symbol	Units	Quantity or equation
Density of seawater	ρ_w	kg m^{-3}	Measured (Shipboard CTD)
Mixed layer depth[a]	MLD	M	$\Delta\sigma_\theta = 0.03$ kg m^{-3}
Wind speed	$U_{3.3\ m}$	m s^{-1}	Measured (WHOTS mooring)
Roughness length	z	m s^{-1}	0.0001
Wind speed	$U_{15\ m}$	m s^{-1}	$U_{15} = U_{3.3} \times \ln(H_1/z)/\ln(H_2/z)$
Density of air	ρ_a	kg m^{-3}	1.2
Drag coefficient[b]	C_D	Dimensionless	1.2×10^{-3}
Wind stress	τ	kg m^{-1} s^{-2}	$\tau = \rho_a \times C_D \times U_{15}^2$
Friction velocity	$u*$	m s^{-1}	$u* = (\tau/\rho_w)^{0.5}$
Turbulent transport velocity	TTV	cm s^{-1}	TTV = dz/dt
Mixing timescale	T	h	T = MLD/TTV

[a]de Boyer Montégut *et al.* (2004).
[b]Large and Pond (1981).

Table IV: Estimates of the temporal variability of PAR irradiance for cells entrained in the motion of the mixed layer

Date	MLD (m)	PAR (5 m)	PAR (MLD)	dPAR/dz (ML)	TTV (m s^{-1})	dPAR/dt (ML)
26 August	18	923.7	475.7	34.46	0	0
28 August	29	712.1	251.7	19.18	0.0037	0.0710
29 August	45	792.4	157.5	15.87	0.0029	0.0460
31 August	40	902.7	209.4	19.81	0.0052	0.1030
1 September	27	912.0	347.2	25.68	0.0048	0.1232

With the exception of 26 August, the R^2 values for the XCP/CHLA gradient regression analyses ranged from 0.667 to 0.856. The average XCP/CHLA value (0.186) measured in the mixed layer on 26 August 2012 exceeded the light-adapted XCP/CHLA values (0.180–0.182) measured during the XCP time-series, and the mixing rate was assumed to be $\approx$ 0 m s^{-1}. For wind speeds >7.5 m s^{-1}, TTVs averaged 0.41 $\pm$ 0.10 cm s^{-1} during H-D 9. Based on these latter rates and the observed mixed layer depths, we estimate the mixing timescale (T) to be 2–4 h.

The process of photoadaptation of XCP/CHLA is triggered by a change of light intensity over time (dPAR/dt) that we did not directly take into account in Eq. (2). In that simplified case, we applied a value of dP/dt calculated from the diel variation of XCP/CHLA at the sea surface (cf. Fig. 5), but we wanted to verify that dPAR/dt from those measurements was comparable to dPAR/dt experienced by the cell being displaced in the mixed layer by the water movement. The temporal variation of light during the diel experiment is given by the difference of PAR between successive data points in Fig. 5, divided by the time distance between those points. We call this first quantity dPAR/dt (diel), and its average value is 0.095 $\pm$ 0.097 μmol quanta m^{-2} s^{-2}. The estimates of the temporal variability of light for cells entrained in the motion of the mixed layer, dPAR/dt (ML), was calculated starting from the average vertical gradient of PAR in the mixed layer, dPAR/dz (ML), and TTV:

$$\frac{\mathrm{dPAR}}{\mathrm{d}t(\mathrm{ML})} = \frac{\mathrm{dPAR}}{\mathrm{d}z(\mathrm{ML})} \times \mathrm{TTV} \qquad (3)$$

We computed dPAR/dz (ML) as the gradient of light between 5 m and MLD using measurements of the vertical attenuation of PAR in the water column (Table IV). The average value of dPAR/dt (ML) is 0.085 $\pm$ 0.034 μmol quanta m^{-2} s^{-2}, considering just the four data points with non-zero TTV. Since dPAR/dt (diel) is very similar to dPAR/dt (ML), we conclude that the value of dP/dt computed from data in Fig. 5 can be applied for the calculation of TTV from the vertical gradients of XCP/CHLA.

D'Asaro (D'Asaro, 2001) used Lagrangian floats to measure vertical velocities for open waters west of Vancouver Island during January 1995. Vertical velocities (σ_w) and friction velocity ($u*$) were tightly correlated and ranged from 0.43 to 3.20 cm s^{-1} and 0.0037 to 0.0276 m s^{-1}, respectively (i.e. $\sigma_w = (1.35)^{0.5}\ u*$). D'Asaro (D'Asaro, 2001) points out that since each float traverses the mixed layer several times during the averaging period of 3.6 h, σ^2_w corresponds approximately to the mixed layer average of the square of the vertical velocity (w^2).The D'Asaro floats are ballasted to be slightly buoyant in order to prevent escape from the mixed layer, and do not perform well below a wind speed of ~8 m s^{-1} (Eric D'Asaro, personal communication). This slight buoyancy difference leads to a non-uniform float distribution in mixed layer. The distribution is skewed toward the surface and becomes more uniform with increasing wind stress. Consequently, the floats oversample the more energetic upper portion of the mixed layer and positively bias the value of $\sigma_w{}^2/u*{}^2$ by a factor of 1.27 for the mixed layer depth average (see text and Fig. 6 in D'Asaro, 2001

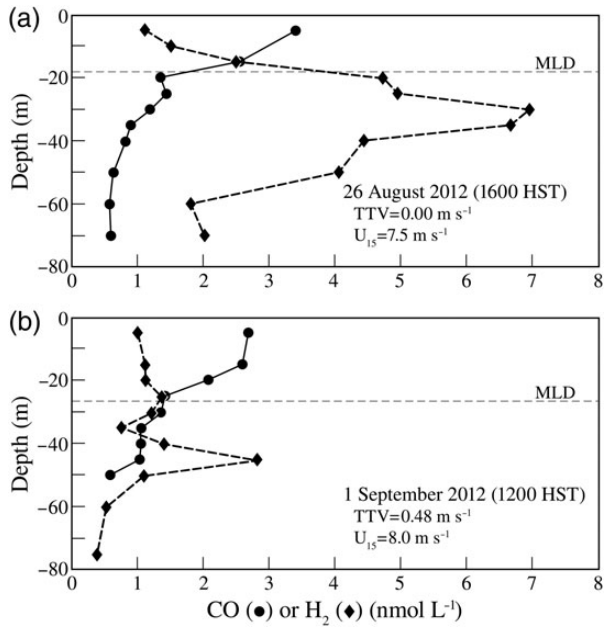

Fig. 7. Vertical distributions of H_2 and CO measured on (**a**) 26 August and (**b**) 1 September during KM1219.

for details). After correcting for Lagrangian float biases, Eric D'Asaro (personal communication) estimates a vertical velocity of 1 cm s^{-1} at a u_* of 0.010 m s^{-1} based on his data set. This value agrees to within a factor of ~2 with the average TTV of 0.41 ± 0.10 cm s^{-1} measured during this study on 28 August–1 September ($n = 4$, $u_* = 0.010 \pm 0.001$ m s^{-1}).

How mixed is the mixed layer: example of trace gas distributions

The timescales of mixing identified from XCP measurements (2–4 h) are similar to the turnover times of H_2 and CO in the mixed layer. The residence time for both H_2 and CO is in general less than a day and most likely on the order of several hours (Doney *et al.*, 1995; Wilson *et al.*, 2013). Under stratified, low-mixing conditions, vertical profiles of CO decrease exponentially causing sharp near-surface gradients in concentration. This was exhibited on 26 August when the low average wind speed and mixing rate resulted in a shallow mixed layer depth of 18 m and sharp gradients of H_2 (0.24 nM m^{-1}) and CO (0.13 nM m^{-1}) were observed in the mixed layer (Fig. 7). In contrast, the higher average wind speed and mixing rate observed on 1 September yielded a deeper mixed layer depth of 27 m and weaker H_2 (0.02 nM m^{-1}) and CO (0.06 nM m^{-1}) gradients in the mixed layer. The pronounced sub-surface maximum in dissolved H_2 observed on 26 August is unusual with respect to its amplitude, exceeding typical surface ocean concentrations by two–three-fold compared with previous measurements of dissolved H_2 in the Pacific Ocean (Moore *et al.*, 2009; Wilson *et al.*, 2013). The sub-surface maximum was not observed during the remainder of the KM1219 cruise and its location just below the mixed layer depth indicates a biological production source, most likely a byproduct of dinitrogen fixation (Wilson *et al.*, 2013). In contrast to H_2 which is produced during the day and night, the production of CO, by the photochemical degradation of chromophoric dissolved organic matter, is a daytime only phenomenon with concentrations decreasing during the night as a result of microbial consumption (Blomquist *et al.*, 2012; Zafiriou *et al.*, 2008). Ultimately, the vertical profiles of CO are in good agreement with the estimates of mixing derived from the XCP measurements for the 26 August and 1 September 2012, and suggest that they can provide an insight into vertical advection over short timescales.

CONCLUSIONS AND FUTURE DIRECTIONS

The results of this study reveal that the measurement of time-dependent variations in chlorophyll *a*-normalized XCP concentrations shows promise for investigating upper ocean mixing processes at Station ALOHA. The use of the diaphragm pumping system allowed the rapid collection of seawater samples on much shorter timescales (minutes) than that observed for changes in XCP concentrations (tens-of-minutes). While the conversion of DDX to DTX can provide information on rates of photoadaptation on timescales of seconds-to-minutes, the rate constant determined for this reaction is much too fast to obtain reliable DES depth profiles with the diaphragm pumping system used in this study. Coincident measurements of H_2 and CO profiles suggest that XCP dynamics may be useful for the interpretation of trace gas distributions in the mixed layer. Future studies should be conducted in the winter months when wind speeds are higher and mixed layer depths deeper in order to determine whether a predictable relationship exists between TTV and friction velocity (cf. D'Asaro, 2001). The latter would permit a reconstruction of turbulent transfer velocities over the last decade using the WHOTS mooring wind speed data, and provide an additional tool for the interpretation of biogeochemical variations at Station ALOHA.

ACKNOWLEDGEMENTS

The authors thank Captain and crew of the R/V *Kilo Moana* for their valuable support during KM1219. We

are grateful to Dan Repeta (Woods Hole Oceanographic Institution) for the use of his diaphragm pumping system, Yoshimi Rii (University of Hawaii) for providing the *Pelagomonas* sp. culture, Ricardo Letelier and Jasmine Nahorniak (Oregon State University) for access to the vertical measurements of spectral irradiance, Susan Brown (University of Hawaii) for the use of the Percival incubator, Robert Weller and Al Plueddemann (Woods Hole Oceanographic Institution) for providing WHOTS mooring wind speed data and finally Roger Lukas (University of Hawaii) and Eric D'Asaro (University of Washington) for providing valuable discussions regarding mixing processes in the upper ocean.

FUNDING

This research was supported by National Science Foundation grants EF-0424599 (D.M.K.) and OCE-1153656 (D.M.K. and S.T.W.), National Oceanic and Atmospheric Administration grant NA09OAR4320129, and the Gordon and Betty Moore Foundation (D.M.K.).

REFERENCES

Andersen, R. A., Bidigare, R. R., Keller, M. D. *et al.* (1996) A comparison of HPLC pigment signatures and electron microscopic observations for oligotrophic waters of the North Atlantic and Pacific Oceans. *Deep-Sea Res. II*, **43**, 517–537.

Bidigare, R. R., Smith, R. C., Baker, K. S. *et al.* (1987) Oceanic primary production estimates from measurements of spectral irradiance and pigment concentrations. *Global Biogeochem. Cycles*, **1**, 171–186.

Bidigare, R. R., Van Heukelem, L. and Trees, C. C. (2005) Analysis of algal pigments by high-performance liquid chromatography. In Andersen, R. A. (ed.), *Algal Culturing Techniques*. Academic Press, New York, pp. 327–345.

Bingham, F. and Lukas, R. (1996) Seasonal cycles of temperature, salinity and dissolved oxygen observed in the Hawaii Ocean Time-series. *Deep-Sea Res. II*, **43**, 199–213.

Blomquist, B. W., Fairall, C. W., Huebert, B. J. *et al.* (2012) Direct measurement of the oceanic carbon monoxide flux by eddy correlation. *Atmos. Meas. Tech. Discuss.*, **5**, 4809–4825.

Brunet, C., Casotti, R., Aronne, B. *et al.* (2003) Measured photophysiological parameters used as tools to estimate vertical water movements in the coastal Mediterranean. *J. Plankton Res.*, **25**, 1413–1425.

Brunet, C., Casotti, R., Aronne, B. *et al.* (2008) Phytoplankton diel and vertical variability in photobiological responses at a coastal station in the Mediterranean Sea. *J. Plankton Res.*, **30**, 645–654.

Brunet, C., Johnsen, G., Lavaud, J. *et al.* (2011) Pigments and photoacclimation processes. In Roy, S., Johnsen, G., Llewellyn, C. and Skarstad, E. (eds.), *Phytoplankton Pigments, Characterization, Chemotaxonomy and Applications in Oceanography. Oceanographic Methodologies, Vol. 2*. SCOR-UNESCO Publishing, Cambridge University Press, p. 880.

Brunet, C. and Lavaud, J. (2010) Can the xanthophyll cycle help extract the essence of the microalgal functional response to a variable light environment? *J. Plankton Res.*, **32**, 1609–1617.

Claustre, H., Kerhervé, P., Marty, J.-C. *et al.* (1994) Phytoplankton photoadaptation related to some frontal physical processes. *J. Mar. Syst.*, **5**, 251–265.

Cullen, J. J. and Lewis, M. R. (1988) The kinetics of algal photoadaptation in the context of vertical mixing. *J. Plankton Res.*, **10**, 1039–1063.

Dambek, M., Eilers, U., Breitenbach, J. *et al.* (2012) Biosynthesis of fucoxanthin and diadinoxanthin and function of initial pathway genes in *Phaeodactylum tricornutum*. *J. Exp. Bot.*, **63**, 5607–5612.

D'Asaro, E. (2001) Turbulent vertical kinetic energy in the ocean mixed layer. *J. Phys. Oceanogr.*, **30**, 3530–3537.

de Boyer Montégut, C., Madec, G., Fischer, A. S. *et al.* (2004) Mixed layer depth over the global ocean: an examination of profile data and a profile-based climatology. *J. Geophys. Res.*, **109**, C12003, doi:10.1029/2004JC002378.

Denman, K. L. and Gargett, A. E. (1983) Time and space scales of vertical mixing and advection of phytoplankton in the upper ocean. *Limnol. Oceanogr.*, **28**, 801–815.

Doney, S. C., Najjar, R. G. and Stewart, S. (1995) Photochemistry, mixing and diurnal cycles in the upper ocean. *J. Mar. Res.*, **53**, 341–369.

Dusenberry, J. A. (1995) Picophytoplankton photoacclimation and mixing in the surface oceans. Ph.D. thesis, Massachusetts Institute of Technology/Woods Hole Oceanographic Institution.

Dusenberry, J. A., Olson, R. J. and Chisholm, S. W. (1999) Frequency distributions of phytoplankton single-cell fluorescence and vertical mixing in the surface ocean. *Limnol. Oceanogr.*, **44**, 431–435.

Ferris, J. M. and Christian, R. (1991) Aquatic primary production in relation to microalgal responses to changing light: A review. *Aquat. Sci.*, **53**, 187–217.

Gargett, A. E. (1997) "Theories" and techniques for observing turbulence in the ocean euphotic zone. *Sci. Mar.*, **61**, 25–45.

Griffith, G. P., Vennell, R. and Williams, M. J. M. (2010) An algal photoprotection index and vertical mixing in the Southern Ocean. *J. Plankton Res.*, **32**, 515–527.

Harris, G. N., Scanlan, D. J. and Geider, R. J. (2009) Responses of *Emiliania huxleyi* (Prymnesiophyceae) to step changes in photon flux density. *Eur. J. Phycol.*, **44**, 31–48.

Kashino, Y. and Kudoh, S. (2003) Concerted response of xanthophyll-cycle pigments in a marine diatom, *Chaetoceros gracilis*, to shifts in light condition. *Phycol. Res.*, **51**, 168–172.

Kashino, Y., Kudoh, S., Hayashi, Y. *et al.* (2002) Strategies of phytoplankton to perform effective photosynthesis in the North Water. *Deep-Sea Res. II*, **49**, 5049–5061.

Large, W. G. and Pond, S. (1981) Open ocean momentum flux measurements in moderate to strong winds. *J. Phys. Oceanogr.*, **11**, 324–336.

Lavaud, J., Rousseau, B. and Etienne, A.-L. (2002) In diatoms, a transthylakoid proton gradient alone is not sufficient to induce a non-photochemical fluorescence quenching. *FEBS Lett.*, **523**, 163–166.

Lepetit, B., Volke, D., Gilbert, M. *et al.* (2010) Evidence for the existence of one antenna-associated, lipid-dissolved and two protein-bound pools of diadinoxanthin cycle pigments in diatoms. *Plant Physiol.*, **154**, 1905–1920.

Lewis, M. R., Cullen, J. J. and Platt, T. (1984) Relationships between vertical mixing and photoadaptation of phytoplankton: Similarity criteria. *Mar. Ecol. Prog. Ser.*, **15**, 141–149.

Lohr, M. and Wilhelm, C. (1999) Algae displaying the diadinoxanthin cycle also possess the violaxanthin cycle. *Proc. Natl Acad. Sci. USA*, **96**, 8784–8789.

Moline, M. A. (1998) Photoadaptive response during the development of a coastal Antarctic diatom bloom and relationship to water column stability. *Limnol. Oceanogr.*, **43**, 146–153.

Moore, R. M., Punshon, S., Mahaffey, C. *et al.* (2009) The relationship between dissolved hydrogen and nitrogen fixation in ocean waters. *Deep-Sea Res.*, **56**, 1449–1458.

Olaizola, M., Bienfang, P. K. and Ziemann, D. A. (1992) Pigment analysis of phytoplankton during a subarctic bloom: Xanthophyll cycling. *J. Exp. Mar. Biol. Ecol.*, **158**, 59–74.

Olaizola, M. and Yamamoto, H. Y. (1994) Short-term response of the diadinoxanthin cycle and fluorescence yield to high irradiance in *Chaetoceros muelleri* (Bacillariophyceae). *J. Phycol.*, **30**, 606–612.

Scharek, R., Latasa, M., Karl, D. M. *et al.* (1999) Temporal variations in diatom abundance and downward vertical flux in the oligotrophic North Pacific gyre. *Deep-Sea Res.*, **46**, 1051–1075.

Welschmeyer, N. A. and Hoepffner, N. (1986) Rapid xanthophyll cycling: an *in situ* tracer for mixing in the upper ocean. EOS. *Trans. Am. Geophys. Union*, **67**, 969.

Wilson, S. T., del Valle, D. A., Robidart, J. C. *et al.* (2013) Dissolved hydrogen and nitrogen fixation in the oligotrophic North Pacific Subtropical Gyre. *Environ. Microbiol. Reports*, doi:10.1111/1758-2229.12069.

Wright, S. W., Jeffrey, S. W., Mantoura, R. F. C. *et al.* (1991) Improved HPLC method for the analysis of chlorophylls and carotenoids from marine phytoplankton. *Mar. Ecol. Prog Ser.*, **7**, 183–196.

Xie, H., Andrews, S. S., Martin, W. R. *et al.* (2002) Validated methods for sampling and headspace analysis of carbon monoxide in seawater. *Mar. Chem.*, **77**, 93–108.

Zafiriou, O. C., Xie, H., Nelson, N. B. *et al.* (2008) Diel carbon monoxide cycling in the upper Sargasso Sea near Bermuda at the onset of spring and in midsummer. *Limnol. Oceanogr.*, **53**, 835–850.